A Thalamo-Hypothalamic Pathway That Activates Oxytocin Neurons in Social Contexts in Female Rats

Melinda Cservenák,[1,2]* Dávid Keller,[1,2]* Viktor Kis,[1,4] Emese A. Fazekas,[1,5] Hanna Öllös,[1] András H. Lékó,[2] Éva R. Szabó,[1,2] Éva Renner,[3] Ted B. Usdin,[6] Miklós Palkovits,[3] and Árpád Dobolyi[1,2]

[1]MTA-ELTE NAP B Laboratory of Molecular and Systems Neurobiology, Department of Physiology and Neurobiology, Hungarian Academy of Sciences and Eötvös Loránd University, Budapest 1117, Hungary; [2]Laboratory of Neuromorphology and [3]MTA-SE NAP Human Brain Tissue Bank Microdissection Laboratory, Department of Anatomy, Histology and Embryology, Semmelweis University, Budapest 1094, Hungary; [4]Department of Anatomy, Cell and Developmental Biology, Institute of Biology, Eötvös Loránd University, Budapest 1117, Hungary; [5]Department of Ethology, Eötvös Loránd University, Budapest 1117, Hungary; and [6]Section on Fundamental Neuroscience, National Institute of Mental Health, Bethesda, Maryland 20892

Oxytocin is released from neurons in the paraventricular hypothalamic nucleus (PVN) in mothers upon suckling and during adult social interactions. However, neuronal pathways that activate oxytocin neurons in social contexts are not yet established. Neurons in the posterior intralaminar complex of the thalamus (PIL), which contain tuberoinfundibular peptide 39 (TIP39) and are activated by pup exposure in lactating mothers, provide a candidate projection. Innervation of oxytocin neurons by TIP39 neurons was examined by double labeling in combination with electron microscopy and retrograde tract-tracing. Potential classic neurotransmitters in TIP39 neurons were investigated by *in situ* hybridization histochemistry. Neurons activated after encounter with a familiar conspecific female in a familiar environment were mapped with the c-Fos technique. PVN and the supraoptic nucleus oxytocin neurons were closely apposed by an average of 2.0 and 0.4 TIP39 terminals, respectively. Asymmetric (presumed excitatory) synapses were found between TIP39 terminals and cell bodies of oxytocin neurons. In lactating rats, PIL TIP39 neurons were retrogradely labeled from the PVN. TIP39 neurons expressed vesicular glutamate transporter 2 but not glutamic acid decarboxylase 67. PIL contained a markedly increased number of c-Fos–positive neurons in response to social encounter with a familiar conspecific female. Furthermore, the PIL received ascending input from the spinal cord and the inferior colliculus. Thus, TIP39 neurons in the PIL may receive sensory input in response to social interactions and project to the PVN to innervate and excite oxytocin neurons, suggesting that the PIL-PVN projection contributes to the activation of oxytocin neurons in social contexts. **(*Endocrinology* 158: 335–348, 2017)**

Oxytocin, as a reproductive hormone of hypothalamic origin, is secreted from the neurohypophysis to evoke uterus contraction and milk ejection in females during parturition and lactation, respectively (1). Oxytocin release within the central nervous system has recently gained major attention as a neuromodulator involved in promoting maternal behaviors (2–4) and social behaviors during nonlactating periods (5, 6). The targets of oxytocin neurons are often limbic areas involved in the social brain network (7, 8). Despite growing

ISSN Print 0013-7227 ISSN Online 1945-7170
Printed in USA

Received 2 September 2016. Accepted 7 November 2016.
First Published Online 14 November 2016

*These authors contributed equally to this work.

Abbreviations: ABC, avidin-biotin-peroxidase complex; c-Fos-ir, c-Fos-immunoreactive; CB, calbindin; CB-ir, calbindin immunoreactive; CTB, cholera toxin β subunit; EM, electron microscopy; FITC, fluorescein isothiocyanate; GAD67, glutamic acid decarboxylase 67; PB, phosphate buffer; PIL, posterior intralaminar complex of the thalamus; PV, parvalbumin; PV-ir, parvalbumin immunoreactive; PVN, paraventricular hypothalamic nucleus; RRID, Research Resource Identifier AB Registry ID; TBS, Tris-buffered saline; TIP39, tuberoinfundibular peptide 39; TIP39-ir, tuberoinfundibular peptide 39 immunoreactive; VGlut2, vesicular glutamate transporter 2.

knowledge of the effects of oxytocin on social interactions (5, 6, 9) and the potential use of the oxytocin system as a drug target [*e.g.*, in autism and eating and addictive disorders (10–12)], surprisingly little information is available on the neuronal inputs leading to the activation of oxytocin neurons (13, 14). A combination of retrograde labeling and the c-Fos technique identified inputs from the A1 and A2 noradrenergic cell groups in the lower brainstem as being important in conveying nociceptive and visceral information to the paraventricular hypothalamic nucleus (PVN) (15, 16). These inputs have also been suggested to mediate the effects of reproductive functions (parturition, lactation) on oxytocin neurons (17). Studies using electrophysiologic and lesion techniques identified the mesencephalic lateral tegmentum and, more rostrally, the ventroposterior thalamic-peripeduncular area as parts of the milk ejection reflex arc (18–20). However, the relay neurons in the milk ejection reflex pathway need to be elucidated. Furthermore, it has not been established how information on social interactions, which can also evoke oxytocin release (21), reaches the oxytocin neurons (13).

A group of neurons in the posterior intralaminar complex of the thalamus (PIL), an area ventromedial to the medial geniculate body, is activated by suckling in lactating female rats (22). The neuropeptide tuberoinfundibular peptide of 39 residues (TIP39) is markedly induced in these neurons immediately after parturition, and in adults TIP39 is highly expressed in this brain region only during the postpartum period (23). TIP39 is the endogenous ligand for the parathyroid hormone 2 receptor (24, 25). TIP39-containing nerve fibers and terminals are abundant in the PVN, where there is a closely matching distribution of the parathyroid hormone 2 receptor (26). Therefore, we hypothesized that TIP39 neurons may be part of an ascending neuronal pathway that innervates and excites oxytocin neurons. To evaluate this hypothesis, we have taken a variety of different approaches for addressing the relationship between TIP39-containing neurons and oxytocin neurons. Retrograde tracing identified neurons in the PIL, many of which contain TIP39, as a major source of projections to the PVN. Furthermore, electron microscopy showed that TIP39 terminals innervate oxytocin neurons. The classic neurotransmitters expressed in TIP39 neurons were also investigated by using a combination of TIP39 immunohistochemistry and *in situ* hybridization histochemistry for vesicular glutamate transporter 2 (VGlut2), a marker of glutamatergic neurons, and glutamic acid decarboxylase 67 (GAD67), a marker of γ-aminobutyric acid–ergic neurons. Because calcium-binding proteins, including calbindin (CB) and parvalbumin (PV), are suitable for defining nuclei and specific cell types within them in the brain (27), including the PIL area, (28-30), we also examined the expression of calcium-binding proteins by PIL TIP39 neurons and in surrounding brain regions so that they could be identified in nonlactating animals when TIP39 is not detectable in the PIL (31). The CB content of these cells helped to determine their activation after encounter of familiar adult females and also in adult–infant interactions. Finally, we injected retrograde tracer into the PIL to reveal the sources of information that activate these neurons during social interactions.

Materials and Methods

Animals

This study was approved by the Animal Examination Ethical Council of the Animal Protection Advisory Board, Semmelweis University, Budapest, Hungary. Procedures involving rats were carried out in accordance with the Hungarian Ministry of Agriculture's Animal Hygiene and Food Control Department guidelines for experimental protocols and with European Union Directive 2010/63/EU for animal experiments. A total of 55 adult female rats (Wistar; Charles Rivers Laboratories, Budapest, Hungary) were used. All of the animals were 90 to 120 days old when euthanized. Animals were kept under standard laboratory conditions with 12-hour light/12-hour dark periods and were supplied with food (VRF1 laboratory chow for rodents, Charles Rivers Laboratories) and drinking water *ad libitum*. Mother rats were housed individually. The number of pups was adjusted to 8 within 2 days of delivery. Rats were anesthetized with 0.2 mL/300 g body weight ketamine (100 mg/mL) and 0.2 mL/300 g body weight xylazine (20 mg/mL).

Tissue collection for light microscopy

Rats were deeply anesthetized and perfused transcardially with 4% paraformaldehyde. Nervous tissue was then transferred to 20% sucrose for 2 days. Serial coronal sections were cut at 50 μm from both the brain and the spinal cord (the latter only for the study aiming the inputs of the PIL) on a sliding microtome (Frigomobil SM 2000 R, Leica Microsystems, Wetzlar, Germany) and collected in phosphate buffer (PB)–containing 0.05% sodium-azide and stored at 4°C. The spinal cord was cut into pieces containing 1 segment before sectioning. The segments were attached to the block by using specimen matrix for cryostat sectioning (Tissue-Tek; Sakura Finetek Europe, Leiden, the Netherlands). The matrix also surrounded spinal cord tissue to provide mechanical stability for sectioning. Sections from different spinal cord segments were collected in different wells of 24-well plates.

Fluorescent double labeling of TIP39 and oxytocin, CB, or PV

Every fourth free-floating brain section was immunolabeled for TIP39. The antiserum (1:3000; Research Resource Identifier AB Registry ID [RRID]: AB_2315466) was applied for 48 hours, followed by incubation of the sections in biotinylated donkey anti-rabbit secondary antibody (1:1000 dilution; Jackson ImmunoResearch, West Grove, PA) and then in avidin-biotin-peroxidase complex (ABC; 1:500; Vector Laboratories, Burlingame, CA) for 2 hours (Table 1). Subsequently, sections

Table 1. Peptide/Protein Targets and Antibodies Used in Study

Peptide/Protein Target	Antigen Sequence (If Known)	Name of Antibody	Manufacturer, Catalog Number, and/or Name of Individual Providing Antibody	RRID	Species Raised in; Monoclonal or Polyclonal	Dilution Used
Mouse/rat tuberoinfundibular peptide of 39 residues	SLALADDAA FRERARLLAAL ERRRWLDSYM QKLLLLDAP	Anti-TIP39	Dr. Ted B. Usdin	AB_2315466	Rabbit, polyclonal	3000×
Oxytocin	CYIQNCPLG	Anti-oxytocin-neurophysin 1 antibody [4G11]	Abcam, ab78364	AB_1603099	Mouse, monoclonal	1000×
CBD-28k		Anti-CB	Sigma-Aldrich, C9848	AB_476894	Mouse, monoclonal	5000×
PV		Anti-PV	Sigma-Aldrich, P3088	AB_477329	Mouse, monoclonal	3000×
CTB		Anti-CTB	List Biological Laboratories, #703	AB_2314252	Goat, polyclonal	10,000×
c-Fos		Anti–c-Fos	Santa Cruz Biotechnology, sc-52;	AB_2106783	Rabbit, polyclonal	20,000×

were treated with fluorescein isothiocyanate (FITC)-tyramide (1:8000) and H_2O_2 in Tris hydrochloride buffer (0.1 M; pH, 8.0) for 6 minutes. Then, mouse antioxytocin (1:1000; ab78364, Abcam, Cambridge, United Kingdom; RRID: AB_1603099), mouse anti-CB D-28k (1:5000; C9848, clone CB-955, Sigma-Aldrich, St. Louis, MO; RRID: AB_476894), or mouse anti-PV antiserum (1:3000; P3088, Sigma-Aldrich; RRID: AB_477329) was applied overnight. Sections were then incubated in donkey Alexa Fluor 594 anti-mouse secondary antibody (Thermo Fisher Scientific, Waltham, MA) for 2 hours.

Microscopy, image processing, and histologic analysis

Sections were examined by using an Olympus BX60 light microscope equipped with fluorescent epi-illumination (Olympus Corp., Tokyo, Japan). Images were captured at 2048 × 2048 pixel resolution with a SPOT Xplorer digital CCD camera (Diagnostic Instruments, Sterling Heights, MI) using 4–40× objectives. Confocal images were acquired with a Zeiss LSM 780 Confocal Microscope System (Carl Zeiss, Thornwood, NY) using 40–63× objectives at an optical thickness of 1 μm for counting varicosities and of 3 μm for cell bodies.

Close appositions were defined as TIP39 varicosities in immediate contact with oxytocin-immunoreactive cells. The numbers of close appositions were counted on individual optical sections. Subsequently, they were checked by maximal-intensity projections to avoid counting them more than once. A total of 30 paraventricular magnocellular, 30 paraventricular parvocellular, and 30 supraoptic oxytocin neurons were evaluated from 3 animals. The section containing the most TIP39-immunoreactive (TIP39-ir) neurons in the PIL was selected from each animal double-labeled for TIP39 and CB or PV. The total number of TIP39-ir neurons with an identifiable cell nucleus and the number of double-labeled cells was counted. Subsequently, the number of single-labeled CB and PV cells was also calculated in the area.

For demonstration purposes, contrast and sharpness of the images were adjusted by using the "levels" and "sharpness" commands in Adobe Photoshop CS 8.0 (Adobe Systems Inc., San Jose, CA). The final versions of images were adjusted to 300 dpi resolution.

Correlated light and electron microscopy for the double labeling of TIP39 and Oxytocin

Unless otherwise stated, all reagents and materials used for electron microscopy (EM) studies were obtained from Sigma-Aldrich. Experimental procedures for EM were carried out at room temperature.

Pre-embedding EM immunohistochemistry

Three rats were deeply anesthetized and perfused through the heart with saline, followed by 500 mL of fixative made up of 4% formaldehyde (Merck, Whitehouse Station, NJ), 0.05% glutaraldehyde, and 0.2% picric acid in PB. Sections 50 μm thick were cut with a vibratome, washed in Tris-buffered saline (TBS) (0.05 M; pH, 7.6), cryoprotected in 30% sucrose in TBS overnight, and freeze-thawed over liquid nitrogen 3 times. After washes and treatment with 1% hydrogen peroxide, the sections were processed for immunostaining using the following protocol: quenching in 50 mM ammonium chloride and 50 mM glycine in TBS for 30 minutes; 2% bovine serum albumin for 1 hour; anti-TIP39 antiserum (1:3000) diluted in 0.5% bovine serum albumin–TBS for 48 hours; biotin-conjugated goat anti-rabbit secondary antibody (1:500; Vector Laboratories) for 1 hour; and ABC at 1:500 (Vector Laboratories) for 1 hour. The immunoperoxidase reaction was developed with nickel-intensified 3,3-diaminobenzidine (DAB). Sections were then processed for a second immunostaining. The same protocol was

carried out except that the primary antiserum was mouse antioxytocin (1:1000; ab78364, Abcam), followed by biotin-conjugated goat anti-mouse secondary antibody (1:500; Vector Laboratories). The second immunoperoxidase reaction was developed with DAB. All sections were postfixed in 0.5% OsO_4-containing 3.5% glucose in 0.1 M Na-cacodylate, followed by *en bloc* staining with half-saturated aqueous uranyl acetate, dehydration in ethanol at increasing concentrations and acetonitrile, and then embedding in Durcupan (Araldite casting resin M, Fluka; Sigma-Aldrich). Sections were embedded on slides and cured for 48 hours at 60°C. Small pieces containing oxytocin-immunoreactive cells in the PVN were reembedded and resectioned at 70 nm with Ultracut Ultratome using an E Stereo Star Zoom (Reichert-Jung, DePew, NY) as described elsewhere (32). Sections were collected on pioloform coated single slot copper grids and stained with lead citrate for 1 min.

Electron microscopic image acquisition and processing

Electron micrographs were taken by a side-mounted Morada CCD camera (Olympus Soft Imaging Solutions) connected to a JEOL 1011 (Peabody, MA) or with an UltraScan 1000 charge-coupled device camera (Gatan, Pleasanton, CA) fitted to a CM100 electron microscope (Philips, Amsterdam, the Netherlands). Brightness and contrast were adjusted in the whole digital images of immunogold labeling by using Adobe Photoshop CS2.

Tracer experiments

Cholera toxin β subunit injections

Retrograde tracer experiments were performed and analyzed as detailed elsewhere (33, 34). Briefly, the retrograde tracer cholera toxin β subunit (CTB; List Biological Laboratories, Campbell, CA) was targeted to the PVN (n = 10) and to the PIL (n = 15) in lactating mother rats at postpartum day 4. For stereotaxic injections, rats were positioned in a stereotaxic apparatus. Holes of about 2 mm in diameter were drilled into the skull above the target coordinates. Glass micropipettes of 15 to 20-μm internal diameter were filled with 0.25% CTB dissolved in PB and lowered to the following stereotaxic coordinates (35): anteroposterior (AP), –1.7 mm; lateral (L), 0.4 mm; ventral (V), 7.4 mm for the PVN; and AP, –5.2 mm; L, 2.6 mm; and V, 6.4 mm for the PIL. CTB was applied by iontophoresis using a constant current source (51413 Precision Current Source; Stoelting, Wood Dale, IL) that delivered a current of +6 μA, which pulsed for 7 seconds on and 7 seconds off for 15 minutes. Then the pipette was left in place for 10 minutes without current and was withdrawn under negative current. After injections, the animals were allowed to survive for 7 days.

Visualization of CTB

Sections were pretreated in PB-containing 0.5% Triton X-100 and 3% bovine serum albumin for 1 hour. Sections were then incubated in goat anti-CTB antiserum (1:10,000; #703, List Biological Laboratories; RRID: AB_2314252) overnight. Then, sections were incubated in donkey Alexa Fluor 594 anti-goat secondary antibody (Thermo Fisher Scientific) for 2 hours.

Double immunolabeling of CTB and TIP39 or CB

Every fourth free-floating section was first stained for TIP39 by using FITC-tyramide amplification fluorescent immunocytochemistry, as described earlier. Sections were then incubated overnight in goat anti-CTB or mouse anti-CB antisera, followed by Alexa594 anti-goat or anti-mouse IgG for 1 hour.

Double labeling of VGlut2 and GAD67 messenger RNA with TIP39

Preparation of probes for VGlut2 and GAD67

Probe preparation and *in situ* hybridization was performed as described previously (26, 36). A 279–base pair–long region of the rat VGlut2 (National Center for Biotechnology Information Reference Sequence: NM_053427.1) and a 354–base pair–long region of the GAD67 (National Center for Biotechnology Information Reference Sequence: NM_017007.1) Complementary DNA sequences were polymerase chain reaction amplified by using the following primers: ATGCCCCTAGCTGGTATCCT and CCTGCAGAAGTTTGCAACAA for VGlut2 and GTGCAGGCTACCTCTTCCAG and ACTCCATCATCAGGGCTTTG for GAD67. The polymerase chain reaction products were subcloned into a TOPO TA vector (Thermo Fisher Scientific) containing a T7 RNA polymerase recognition site. The T7 promoter was used to generate [^{35}S]uridine triphosphate–labeled riboprobes, with a MAXIscript transcription kit (Ambion, Austin, TX), according to the kit instructions.

Combination of in situ *hybridization and immunohistochemistry*

Brains of 3 lactating mother rats on day 11 postpartum were dissected and frozen. Then, serial coronal sections (12 μm) were cut, mounted immediately, dried, and stored at −80°C until use. Tissue was prepared by using an mRNAlocator Kit (Ambion), according to the manufacturer's instructions. For hybridization, we used 80 μL hybridization buffer and 1 million decay per minute of labeled probe per slide. Washing procedures included a 30-minute incubation in RNase A followed by decreasing concentrations of sodium-citrate buffer (pH, 7.4) at room temperature and then at 65°C. Subsequently, the slides were immunolabeled for TIP39 by using the peroxidase technique. The rabbit anti-TIP39 antiserum described previously was applied at 1:1000 dilution for 24 hours in a humidified chamber and stained as described earlier. Then, slides were dipped in nuclear track beta nuclear track emulsion (Eastman Kodak, Rochester, NY); stored for 3 weeks at 4°C for autoradiography, developed and fixed with Kodak Dektol developer and Kodak fixer, respectively; and coverslipped.

c-Fos activation study

Social interaction experiment

Female rat littermates (n = 8) grown up together (housed 2 per cage) were used in the study. The 2 rats were separated for 22 hours to reduce basal c-Fos activation. Then, the 2 rats were reunited again in the cage they had cohabited. Control females continued to be kept separately. All animals were euthanized 24 hours after the beginning of separation (*i.e.*, 2 hours after reunion of the socially interacting group). Animals were then processed for c-Fos and CB immunohistochemistry.

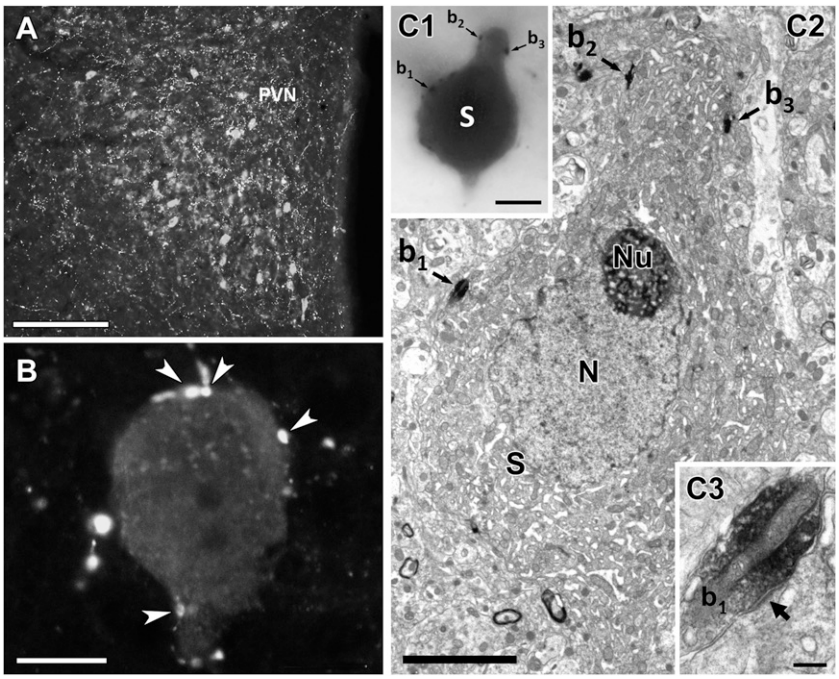

Figure 1. Innervation of oxytocin neurons by TIP39 terminals. (A) TIP39-ir terminals (white) in the PVN overlap with the location of oxytocin-immunoreactive (oxytocin-ir) neurons (gray). (B) The high-magnification confocal image demonstrates that TIP39-ir varicosities closely appose cell bodies and proximal dendrites of oxytocin-ir cell bodies. The white arrowheads point to close appositions. (C) Correlated light microscope and EM evidence of synaptic connection between TIP39-ir terminals and oxytocin neurons in the anterior part of magnocellular PVN. (C1) Black TIP39-ir boutons (b_{1-3}) closely appose an oxytocin-ir cell (gray). (C2) The positions of the 3 boutons are shown in an EM image of the same cell as in C1. (C3) The high-magnification EM image demonstrates an asymmetric synaptic contact between a bouton (b_1) and the cell body of the oxytocin-ir neuron. The black arrow points to the postsynaptic density. N, nucleus; Nu, nucleolus; S, soma. Scale bar = 200 μm for (A), 20 μm for (B), 20 μm for (C1), 20 μm for (C2), and 300 nm for (C3).

Pup exposure of mother rats

Rat dams (n = 8) were deprived of pups on postpartum day 8 to 9 at 11:00. The following day at 09:00, pups were returned to the cage of 4 mother rats. All mothers accepted the pups and suckling started within 5 minutes. Control dams were not united with their litters. All animals were euthanized 24 hours after removal of the pups (*i.e.*, 2 hours after the pups were returned to the mothers).

c-Fos immunohistochemistry

Every fourth free-floating section of the 4 brains per group was immunolabeled as described above for CTB with immunoperoxidase labeling with nickel-intensified DAB except that a rabbit anti-c-Fos primary antiserum (1:20,000; c-Fos [4] sc-52; Santa Cruz Biotechnology, Santa Cruz, CA; RRID: AB_2106783) was used.

Double immunolabeling of c-Fos and CB

One set of every fourth free-floating section from the 8 female rats used for single labeling of c-Fos was double immunolabeled for c-Fos and CB. Then, sections were placed in rabbit antic-Fos primary antiserum (1:20,000) for 24 hours, followed by incubation of the sections in biotinylated donkey anti-rabbit secondary antibody (1:1000; Jackson ImmunoResearch) and then in ABC (1:500; Vector Laboratories) for 1 hours. Subsequently, sections were visualized with FITC-tyramide. Then, the mouse anti-CB D-28k antiserum and donkey Alexa Fluor 594 anti-mouse secondary antibody (Thermo Fisher Scientific) were applied.

Analysis of c-Fos and CB immunolabeling

The section containing the most c-Fos-immunoreactive (c-Fos-ir) neurons in the PIL was selected from each of the 8 animals, and a picture was taken of it. The total number of c-Fos-ir neurons in the PIL of these images was counted by using ImageJ software, version 1.47 (National Institutes of Health, Bethesda, MD). An algorithm, based on intensity, size, and circularity thresholding, was used for all images to select the c-Fos-ir nuclei, whose number was counted automatically by the program. Specifically, color images (2048 × 2048 pixels) containing the entire PIL were photographed such that no saturated pixels were present. Subsequently, the color images were first converted to 8-bit black-and-white images using ImageJ version 1.47. Then, spots were selected whose brightness intensity value was <150 (between 0 and 150 on the 0-to-255 scale). The number of c-Fos–containing cells was defined as the number of selected spots counted in a size ranging from 20 to 100 pixels, and a circularity factor between 0.5 and 1.0. Statistical analyses were performed by using Prism 5 for Windows (GraphPad Software, La Jolla, CA). The number of c-Fos-ir neurons in the 2 groups was compared by using the Student *t* test.

For the analysis of double labeling of c-Fos and CB, confocal images were obtained. Randomly selected 30 c-Fos–positive neurons were used in the analysis. c-Fos–positive neurons were considered double-labeled if CB immunoreactivity was visible around the c-Fos–positive nucleus in a single 3-μm-thick optical plane.

Results

Innervation of oxytocin neurons by TIP39-ir axon terminals

Within the anterior hypothalamus, the PVN and supraoptic nucleus receive a dense innervation by TIP39-containing fibers. In both nuclei, the distribution of TIP39 fibers overlapped with the distribution of oxytocin neurons [Fig. 1(A)]. We also found that most oxytocin neurons were closely apposed by TIP39-containing varicosities [Fig. 1(B)]. The average (standard error of the mean) number of close appositions on the soma and proxymal dendrites of oxytocin neurons was 2.28 ± 0.38 on parvocellular paraventricular, 1.90 ± 0.39 on magnocellular paraventricular, and 0.42 ± 0.20 on supraoptic

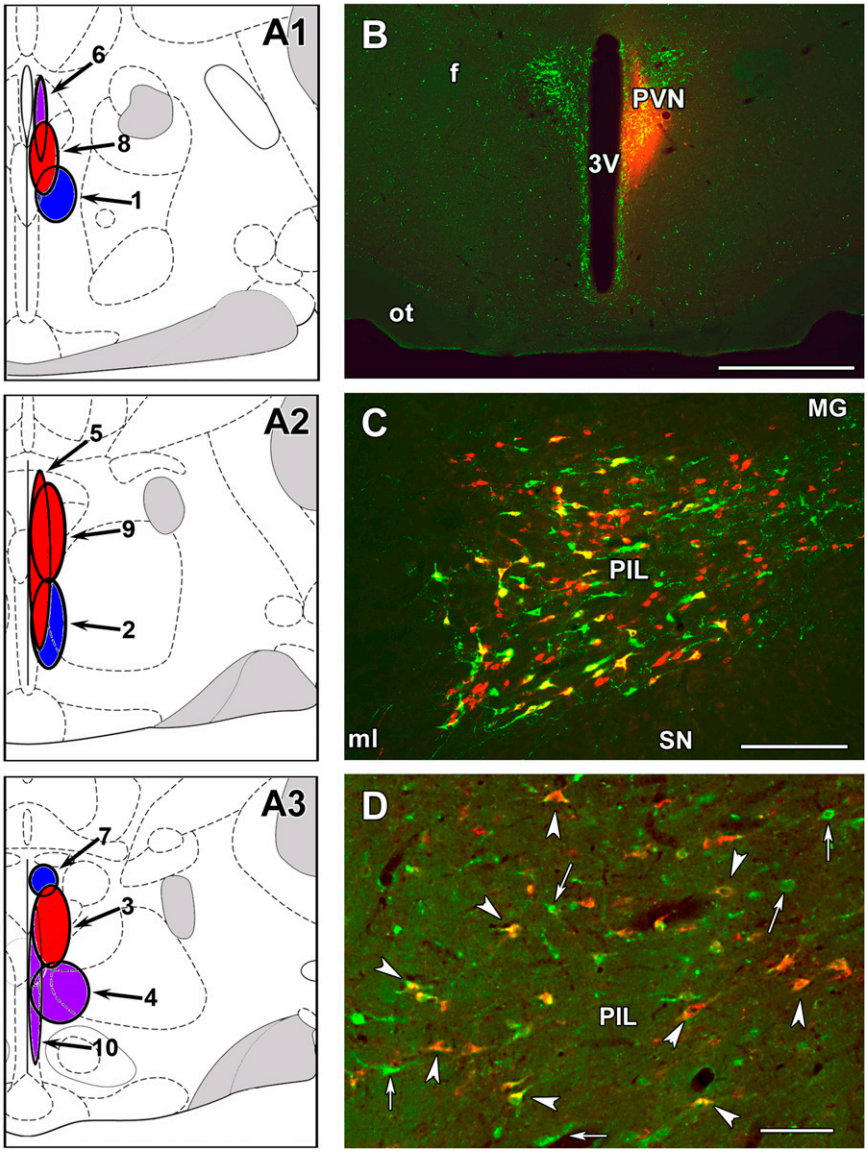

Figure 2. Projection of the PIL to the PVN. (A) The sites where the retrograde tracer CTB spread in the coronal plane following injections in particular animals are circled. Drawings were prepared by aligning the pictures with corresponding schematics adapted from a rat brain atlas (35). The 3 drawings represent coronal sections at bregma levels −1.2 mm, −1.6 mm, and −1.8 mm. The injection sites are shown at the level closest to the center of the injection. The numbers connected to the injection sites by arrows represent the number of the particular animal in the experiment. Injection sites with red, purple, and blue represent many, few, and no retrogradely labeled cells in the PIL, respectively. (B) The injection site of rat 9 is shown for demonstration purposes. The spread of CTB (red) overlaps with a great portion of TIP39-ir fibers (green) located in the PVN. (C) A high number of retrogradely labeled CTB-ir neurons (red) are visible among the TIP39-ir (green) neurons in the ipsilateral PIL. A high percentage of the retrogradely labeled neurons are double-labeled as indicated in yellow. (D) Essentially all CTB-ir neurons (red) are labeled with CB (green) as well. Some examples are shown by white arrowheads. Single-labeled CB-ir neurons are also visible (white arrows). 3V, third ventricle; CTB-ir, CTB-immunoreactive; f, fornix; MG, medial geniculate body; ml, medial lemniscus; ot, optic tract; SN, substantia nigra. Scale bar = 1 mm for (B); 300 μm for (C), and 100 μm for (D).

oxytocin neurons. Correlated light microscopy and EM proved that TIP39-positive thalamic axons innervate oxytocin neurons in the PVN [Fig. 1(C)]. These synapses were all conventional asymmetrical (putative glutamatergic) connections.

Retrograde labeling in PIL following tracer injections into PVN

To identify the source of its TIP39 innervation, we injected the retrograde tracer CTB into the PVN. There were 4 injections with a large overlap between the area of tracer deposition and the territory occupied by TIP39 fibers within the PVN of animals 3, 5, 8, and 9 in Figure 2. The pattern of retrogradely labeled cells was similar for these injections, including several CTB-ir neurons in the ipsilateral medial amygdaloid nucleus, the lateral septum, the bed nucleus of the stria terminalis, several hypothalamic regions, and the lateral parabrachial nucleus (Table 2). In addition, all these injections resulted in many labeled neurons in the PIL. A predominantly ipsilateral labeling of cells was distributed uniformly throughout the PIL, but there were no labeled cells in adjacent brain regions [Fig. 2(C)]. Double labeling showed that 45% of the CTB-labeled neurons in the PIL contained TIP39 immunoreactivity. In addition, essentially all PVN-projecting PIL neurons contained CB [Fig. 2(D)]. Animals 4, 6, and 10, whose injection site only partially overlapped with the PVN, contained few CTB-immunoreactive cells in the PIL, whereas CTB-labeled cells were not present in the PIL in animals 1, 2, and 7; this finding correlated with the fact their injection site missed the PVN.

Chemoarchitecture in thalamic PIL

VGlut2 messenger RNA (mRNA) was present in many parts of the posterior thalamus and rostral midbrain, including the PIL and adjacent structures [Fig. 3(A)]. VGlut2 mRNA appeared evenly distributed within the PIL. Double labeling with TIP39 immunoractivity indicated that essentially all TIP39-ir neurons expressed VGlut2 [Fig. 3(B)]. VGlut2-expessing neurons that did not contain TIP39 immunoreactivity were also abundant. The distribution of GAD67-expressing neurons was distinct from that of VGlut2. For instance, GAD67 was not expressed in the medial geniculate body. GAD67 mRNA was present in all parts

Table 2. Brain Areas Containing Retrogradely Labeled Cells Following CTB Injection Into PVN

Area	Density
Forebrain limbic areas	
Medial prefrontal cortex	++
Medial amygdaloid nucleus	+++
Medial septal nucleus	0
Lateral septal nucleus	+++
Bed nucleus of the stria terminalis	+++
Hypothalamus	
Medial preoptic area	+++
Lateral preoptic area	+
Lateral hypothalamic area	++
Dorsomedial nucleus	++
Ventromedial nucleus	+++
Arcuate nucleus	+
Supramamillary nucleus	++
Mamillary nucleus	+++
Thalamus	
Subparafascicular area	++
Posterior intralaminar thalamic nucleus	+++
Medial geniculate body	0
Midbrain	
Periaqueductal gray	++
Deep mesencephalic nucleus	+
Superior colliculus	0
Inferior colliculus	0
Pons	
Medial parabrachial nucleus	+
Lateral parabrachial nucleus	+++
Cerebellum	0

Brain regions where we did not observe labeled cells are not included or are noted as having a density of 0. +, 1–5 cells per section; ++, 6–15 cells per section; +++, >15 cells per section.

of the PIL, and some adjacent structures, including the anterior pretectal nucleus, and substantia nigra [Fig. 3(C)]. Double labeling of GAD67 mRNA and TIP39 immunohistochemistry indicated that TIP39 neurons do not express GAD67 [Fig. 3(D)].

We investigated the distribution of calcium-binding proteins in and around the PIL to improve the demarcation of the area. Ventral, medial, dorsomedial, and dorsolateral borders of the PIL can be identified by PV-immunoreactive cell bodies in adjacent structures [Fig. 4(A)]. In contrast, the lateral and dorsal borders of the PIL made up the peripeduncular area and the triangular subdivision of the posterior thalamic nucleus cannot be differentiated by using PV immunohistochemistry because they contain few PV-immunoreactive cell bodies and fibers, as does the PIL [Fig. 4(A)]. TIP39-ir neurons, evenly distributed within the PIL [Fig. 4(B)], differentiate it from the peripeduncular area and the triangular subdivision of the posterior thalamic nucleus, which do not contain TIP39-ir cell bodies.

The distribution of CB immunoreactivity is in sharp contrast to that of PV immunoreactivity in and around the PIL. The PIL contains a high density of CB-immunoreactive (CB-ir) cell bodies. Other brain regions adjacent to the PIL contain only few CB-ir cell bodies [Fig. 4(C)]. Within the PIL, both TIP- and CB-ir cell bodies are evenly distributed [Fig. 4(D)]. Furthermore, almost all TIP39-ir neurons contain CB immunoreactivity. CB-positive but TIP39-negative neurons are also present in the PIL [Fig. 4(D)] and outnumber TIP39 neurons by a factor of 2.

Assessment of c-Fos activation in PIL of socially interacting females

Female littermates housed together were separated for 22 hours to reduce basal c-Fos activity. When females were reunited for 2 hours after the 22-hour separation, they engaged in social interactions, including a combined 1 minute of sniffing and 5 minutes of grooming. For about a combined 1 hour, the animals had direct body contact by lying next to each other; during that time, they were seemingly sleeping for about 20 minutes. The rest of the time, they were not in contact while lying, eating, drinking, and grooming on their own. These behaviors were associated with a significantly elevated number of c-Fos-ir neurons in the PIL [Fig. 5(A)] as compared with rats that were kept separated [Fig. 5(B)]. c-Fos-ir neurons appeared evenly distributed within the PIL. Their distribution overlapped with that of the CB-ir neurons [Fig. 5(C)]. In fact, most (86%) c-Fos-ir neurons contained CB [Fig. 5(D)]. The number of c-Fos-ir neurons in the PIL section with the largest number of labeled cells was 169 ± 14 after social interaction with a familiar female, compared with only 41 ± 8 in the separated group; this represents a highly significant increase ($P < 0.001$). The activation of cells in the PIL was specific; adjacent structures did not show an increase in the number of c-Fos-ir neurons. In fact, an elevated number of c-Fos-ir neurons was observed in only a relatively small number of brain regions in interacting mothers, including the medial prefrontal cortex and the amygdala.

In response to suckling, a similar number of activated neurons was present in the PIL of mother rats 2 hours after the pups were returned to them [Fig. 5(E)], calculated as 161 ± 10 (23). The ratio of CB-containing c-Fos–positive cells was 85% of the activated neurons in the PIL of mothers [Fig. 5(F)]. Additional brain areas were also activated in mothers (*e.g.* the medial prefrontal cortex, the lateral septal nucleus, the medial preoptic area, the periaqueductal gray, and the medial paralemniscal nucleus), in agreement with previous literature (37–39).

Projections to PIL

We injected the retrograde tracer CTB into the PIL to identify the neurons that project to it and used injections into adjacent regions for comparison [Fig. 6(A–D)]. Injections that did not overlap the PIL, including into

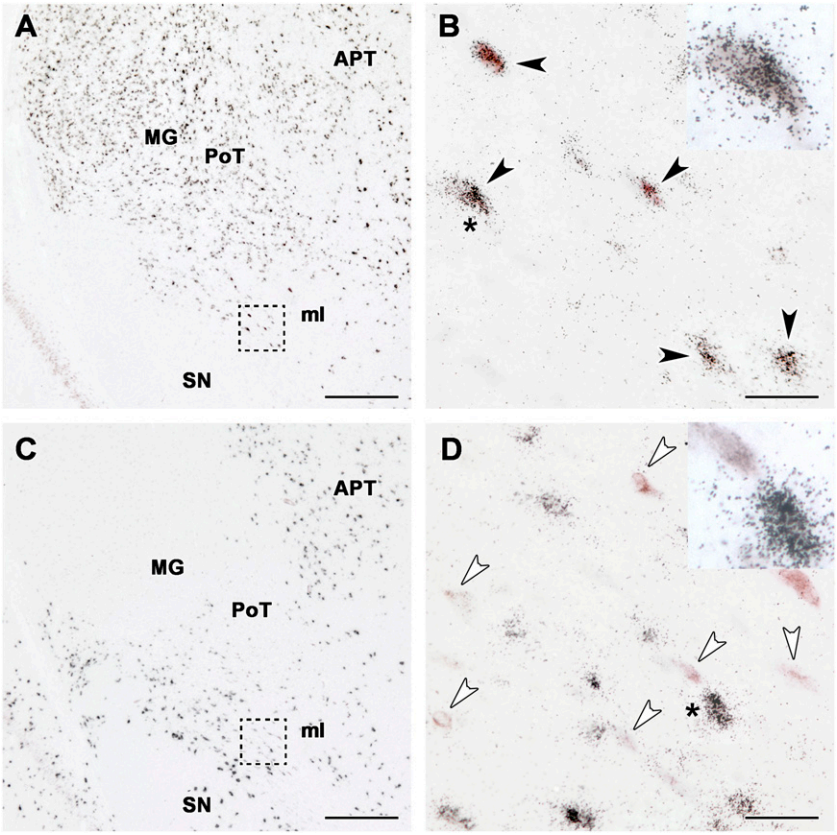

Figure 3. The glutamatergic nature of TIP39 neurons in the PIL. (A) Image of a section labeled with *in situ* hybridization histochemistry for VGlut2 shows the distribution of VGlut2 mRNA expression in the PIL and surrounding brain regions. Note the particularly abundant expression in the medial geniculate body (MG). (B) The framed area in (A) is shown by the high-magnification image, which demonstrates that TIP39-ir cell bodies (brown) contain VGlut2 mRNA as black autoradiographic grains are accumulated above the cells. The double-labeled cells are indicated by black arrowheads. Inset in the upper right corner is magnified image of the double-labeled cell indicated by the star. (C) The distribution of GAD67 mRNA is shown in the PIL and surrounding brain regions. Note the lack of GAD67 mRNA in the MG. (D) The framed area in C is enlarged to demonstrate that TIP39-ir neurons in the PIL (brown) do not express GAD67 in the PIL. The single-immunolabeled neurons are indicated by white arrowheads. Inset in the upper right corner is a magnified image of 2 single-labeled cells whose position is indicated by the star symbol. APT, anterior pretectal area; ml, medial lemniscus; PoT, triangular subdivision of the posterior thalamic nucleus; SN, substantia nigra. Scale bar = 500 μm for (A and C) and 50 μm for (B and D).

varying parts and amounts of the substantia nigra, triangular subdivision of the posterior thalamic nucleus, medial lemniscus, and peripeduncular nucleus, resulted in labeling patterns markedly different from those following PIL injections and generally lacked labeling in areas that were labeled by PIL injections. Most cells projecting to the PIL were ipsilateral to the injection side, except for the gracile and cuneate nuclei and the spinal cord, where there was a contralateral dominance.

Inputs from lower brain regions and spinal cord

The spinal cord contained CTB-labeled neurons contralateral to the injection site. These neurons were distributed in Rexed laminae IV to VI throughout the thoracic and lumbar segments that were sectioned. The cells were typically located in laminae IV to V in thoracic segments [Fig. 6(E)] and laminae V to VI in lumbar segments [Fig. 6(F)]. We rarely found more than 1 labeled cell in a coronal section; on average, every fourth coronal spinal cord section contained a labeled cell. The labeled cells usually had oval perikarya with multiple dendrites [Fig. 6(E and F)].

In the medulla oblongata, the gracile and cuneate nuclei had the highest density of CTB-containing cells [Fig. 6(G)]. The spinal trigeminal nucleus, particularly the deep layers of its ventral portion, also contained a substantial number of labeled cells [Fig. 6(G)]. In these nuclei, the CTB-labeled neurons were located contralateral to the injection site. Only a few regions in the upper brainstem contained any CTB-positive neurons. The highest number of labeled cells was in the external cortex of the inferior colliculus [Fig. 6(H)], and the lateral parabrachial nucleus, the periaqueductal gray, and the deep layers of the superior colliculus contained a low number.

Inputs from higher brain regions

Within the cerebral cortex, the auditory areas contained a considerable number of retrogradely labeled neurons. The insular cortex and the medial prefrontal cortex contained a few CTB-positive neurons, with the highest density of labeled cells in the infralimbic cortex. Other cortical areas were devoid of CTB signal. Retrograde labeling was also absent from most other forebrain structures. We detected a substantial number of labeled neurons only in the central amygdaloid nucleus, the substantia innominata, and the anterior portion of the lateral septal nucleus. Within the diencephalon, the largest number of labeled cells was within the ventromedial hypothalamic nucleus, particularly in its ventrolateral subdivision [Fig. 6(H)]. A considerable number of CTB neurons were also located in the lateral preoptic area and the zona incerta.

Discussion

PIL and its afferent neuronal connections

The PIL, defined by the area containing TIP39 neurons in mother rats, includes the posterior intralaminar

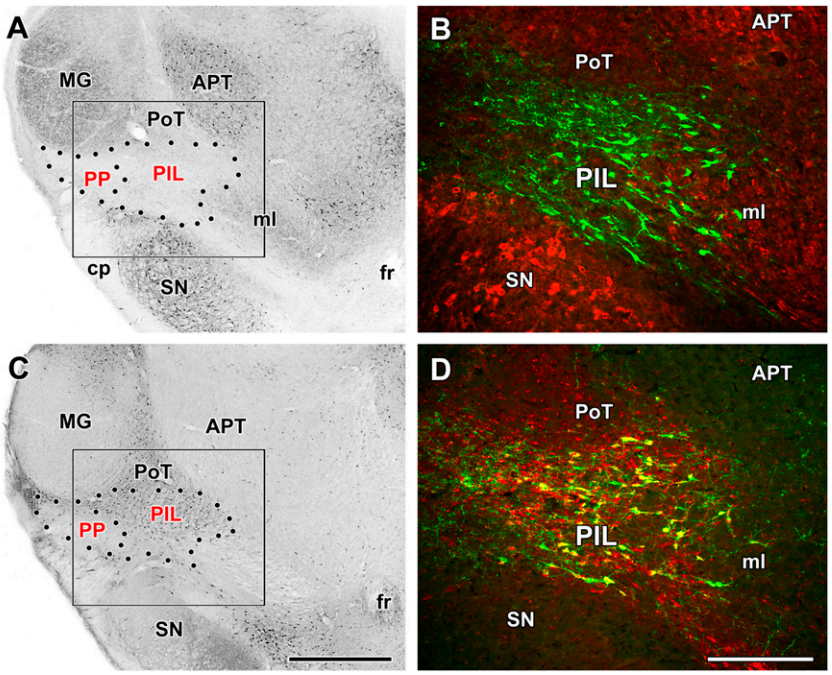

Figure 4. Chemical topography of the PIL. (A) Localization of PV-immunoreactive (PV-ir) neurons in the area. PV-ir neurons are abundant in the anterior pretectal area (APT) and in the substantia nigra (SN). In addition, a high density of PV-ir fiber terminals is present in the medial geniculate body (MG), whereas only a few labeled terminals are found in the PIL, the peripeduncular area (PP), and the triangular subdivision of the posterior thalamic nucleus (PoT). (B) The fluorescent image of a section double-labeled with PV (red) and TIP39 (green) corresponding to the framed area in A indicates that the distribution of TIP39 neurons does not overlap with that of PV-ir neurons, as TIP39 neurons are confined to the PIL. (C) Localization of CB-ir neurons in and around the PIL. CB-ir neurons are present in the PIL and PoT but are absent in the MG, APT, SN, and PP. (D) Fluorescent image of a section double-labeled with CB (red) and TIP39 (green) corresponding to the framed area in (C) indicates that the distribution of TIP39 neurons overlap with that of CB-ir neurons in the PIL but not in the PoT. It is also apparent that most TIP39 neurons express CB (double labeling appears yellow). Scale bar = 1 mm for (C) and 400 μm for (D).

thalamic nucleus and also the parvicellular subparafascicular nucleus and some parts of the caudal subdivision of the zona incerta (26). In this brain area, CB-ir neurons were confined to the PIL except for the triangular subdivision of the posterior thalamic nucleus dorsally adjacent to the PIL, which contains CB-ir neurons but not TIP39 neurons. The distribution of CB immunoreactivity in this study was the same as reported previously in the area but was called the parvocellular part of the subparafascicular nucleus (27, 29). The PIL also corresponds to the posterior intralaminar complex, described as containing CB but not PV in the mouse (28, 30).

On the basis of the data obtained from injections of retrograde tracer into the PIL, identified by the presence of TIP39 neurons, the PIL receives substantial ascending projections. These include direct projections from the contralateral spinal cord as well as indirect projections *via* the gracile and cuneate nuclei. The direct projections arise from throughout the thoracic and lumbar segments and mostly from neurons in deep layers of the dorsal horn of the spinal cord. Additional input arrives from the auditory cortex and the external cortex of the inferior colliculus, a nontonotopically organized auditory nucleus with strong input from the auditory cortex and the spinal trigeminal nucleus (40). In addition, the PIL also receives some descending input from the hypothalamus, particularly from the lateral preoptic area and the ventrolateral subdivision of the ventromedial hypothalamic nucleus. This pattern of PIL afferent connections is similar to that described for neuronal inputs to the parvicellular subparafascicular nucleus in male rats, where the ascending inputs were implicated in the processing of sensory information related to mating and ejaculation (41). Because the PIL includes the parvicellular subparafascicular nucleus, located ventromedial to the medial geniculate body, our results confirm previous data on the afferent neuronal connections of the PIL and expand the results to mother rats with injection sites verified by TIP39 double labeling.

PIL-PVN neuronal pathway and its characteristics

Tha high number of labeled neurons in the PIL following injection of retrograde tracer into the PVN suggests massive input of PIL neurons to the PVN. This pathway specifically connects the PIL with the PVN as neurons were not labeled outside the PIL. In turn, injections into brain areas adjacent to the PVN did not label the PIL. Several previous studies have sought to identify the neuronal inputs to the PVN. Many of them failed to describe the PIL, even though our labeling pattern following PVN injections was essentially the same as reported previously (15, 42–45). We believe that the reasons include the previously poorly defined cyto- and chemoarchitecture of the area, as well as the fact that it is situated at the border of the forebrain and the hindbrain, where some sections can be lost during standard sectioning of the brain for anatomic mapping. Nevertheless, the projection from the PIL to the PVN has been previously shown by using both retrograde and anterograde tracers (46). In that study, the area projecting to the PVN was called the parvicellular division of the subparafascicular and posterior intralaminar nuclei. Thus, in the current study, we confirmed the existence of this pathway. We also showed that some of the PVN

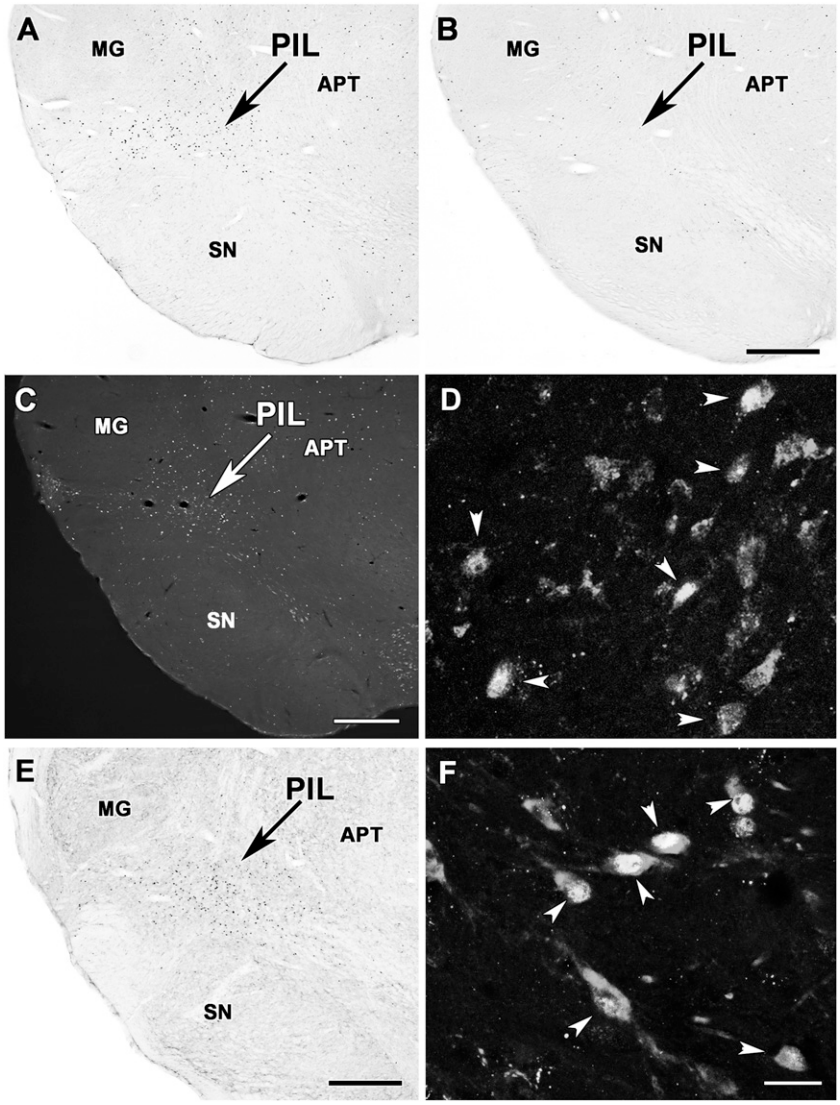

Figure 5. c-Fos immunoreactivity in the PIL in response to social interactions. (A) c-Fos activation in neurons of familiar female rats in familiar environment. c-Fos-ir neurons (black dots) are abundant in the PIL 2 hours after reuniting of rats that were housed together and then separated for 22 hours. The adjacent medial geniculate body (MG) and substantia nigra (SN) are almost completely devoid of c-Fos activation, whereas a lower density of labeled cells is visible in the anterior pretectal nucleus (APT). (B) In animals not reunited with each other, only a few c-Fos–labeled neurons are present in the PIL. (C) The distribution of c-Fos-ir cell nuclei completely overlaps with that of the CB-ir cell bodies in the PIL upon social interactions. (D) High-magnification confocal image demonstrates that most c-Fos-ir neurons contain CB immunoreactivity, indicated by white arrowheads. (E) c-Fos activation in neurons of mother rats. c-Fos-ir neurons (black dots) are abundant in the PIL 2 hours after reuniting of mother rats with their litter following a 22-hour separation period. The distribution of c-Fos-ir cells is similar to that of reunited familiar adults (A). (F) High-magnification confocal image demonstrates that most c-Fos-ir neurons that appeared in mother rats in response to their litter contain CB immunoreactivity. These cells are indicated by white arrowheads. Scale bar = 500 μm for (B, C, and E) and 30 μm for (D and F).

projecting cells contain TIP39. These results are also consistent with previous lesion studies that suggest hypothalamic projections from PIL TIP39 neurons (47).

The current study also showed that the retrogradely labeled neurons have an even distribution within the PIL, further suggesting that the PIL is a topographic unit, even though it does not correspond to an obvious cytoarchitectonically defined nucleus. Retrograde tract-tracing from the PVN also demonstrated that TIP39 neurons constitute a substantial portion of the projection neurons in the PIL. Although TIP39 neurons contain CB, most PVN-projecting TIP39-negative PIL cells are also CB-positive.

The EM study proved that TIP39-containing neurons innervate oxytocin neurons in mother rats. In fact, the average of 2 synaptic connections on the cell body and proxymal dendrites of PVN oxytocin neurons suggests a very robust action of TIP39 neurons on the oxytocin system. Indeed, the receptor for TIP39, the parathyroid hormone 2 receptor, has been previously shown to be particularly abundant in the PVN (48, 49). TIP39 increases cyclic adenosine monophosphate and Ca^{2+} levels by activating the parathyroid hormone 2 receptor *in vitro* (50), which suggests that the neuropeptide has an excitatory action. It is likely that the neurons that contain TIP39 also innervate oxytocin neurons when they do not contain TIP39, such as in nonmaternal (*e.g.* nulliparous) rats. Since we demonstrated that TIP39 cells express VGlut2 and that synapses between TIP39 terminals and oxytocin neurons have asymmetric morphology, TIP39 terminals use the excitatory amino acid transmitter glutamate. Thus, when TIP39 is not present in the terminals of PIL neurons (nonmaternal animals), glutamate is still likely to be present and to exert an excitatory action on oxytocin neurons. Signaling by the PIL to oxytocin neurons in nonmaternal animals may promote social behaviors *via* glutamate release. Co-released TIP39 may potentiate the effect of glutamate in maternal rats. Although we did not address this in this study, we speculate that PVN-projecting CB-positive but TIP39-negative neurons may also innervate oxytocin neurons, similar to TIP39 cells of the PIL, and also provide an excitatory input. TIP39-positive and TIP39-negative CB cells may be part of the same population, with the expression of TIP39 reflecting the strength of the TIP39-inducing stimulus.

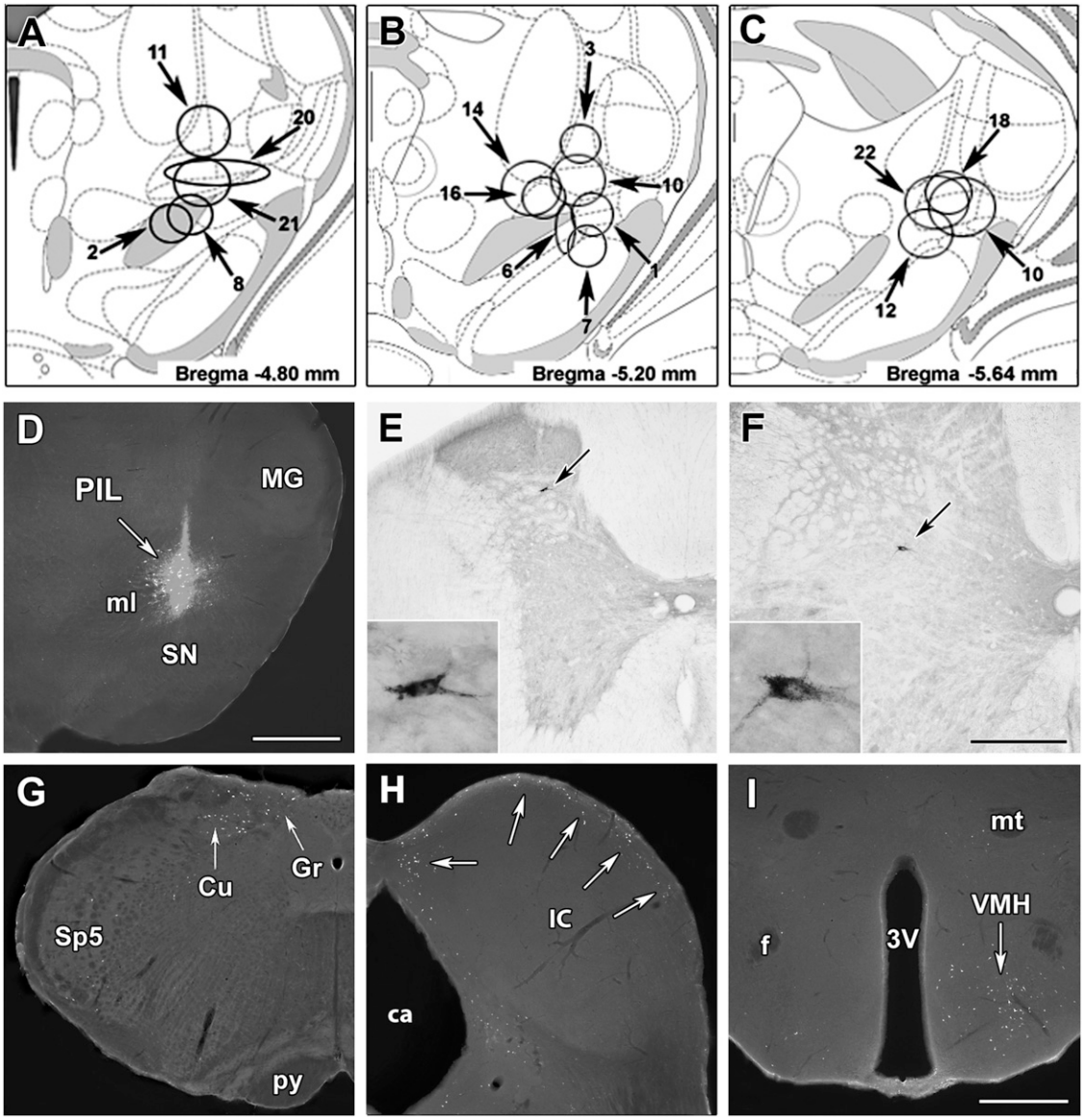

Figure 6. Afferent neuronal connections of the PIL (PIL). (A–C): Sites where the retrograde tracer CTB spread in the coronal plane following injections in particular animals are circled. Drawings were prepared by aligning the pictures adapted from a rat brain atlas (35). The 3 drawings represent coronal sections at bregma levels of −4.8 mm, −5.2 mm, and −5.64 mm. The injection sites are shown at the level closest to the center of the injection. (D) The injection site belonging to animal 10 is shown double-labeled with TIP39 to show that CTB injection site (gray) overlaps with the location of TIP39 neurons (white) in the PIL. (E–I) CTB-labeled cell bodies are shown in the spinal cord at the level of thoracic segment 2 (E) and lumbar segment 5 (F), as well as in different brain regions, including the gracile (Gr) and cuneate (Cu) nuclei in the medulla oblongata (G), the external cortex of the inferior colliculus (H), and the ventromedial hypothalamic nucleus (VMH), especially its ventrolateral subdivision (I). 3V, third ventricle; f, fornix; LV, lateral ventricle; MG, medial geniculate body; mL, corpus callosum; ml, medial lemniscus; mt, mamillothalamic tract; py, pyramidal tract; SN, substantia nigra; Sp5, spinal trigeminal nucleus. Scale bars = 400 μm for (F) and 1 mm for (D and I).

However, our results cannot exclude that they are different cell groups, which innervate different neuron populations in the PVN. We firmly established the existence of an excitatory pathway that projects from the PIL to the PVN and that is available to activate oxytocin neurons in lactating and nonlactating rats (Fig. 7).

Potential functions of PIL-oxytocin neuron connection

The PIL receives ascending inputs, which relay sensory information from the spinal cord. These afferent connections are candidates to convey suckling information from the nipples and the somatosensory components of social contacts to the PIL. Indeed, c-Fos-expressing neurons were described in response to suckling in deep layers of the spinal cord dorsal horn at thoracic and lumbar segments, suggesting that these neurons may relay the suckling information to brain centers (51). In the current study, the activation of CB neurons in the PIL was demonstrated in a social context. Because the female rats were siblings and grew up together, their encounter in the familiar environment is not likely to evoke stress.

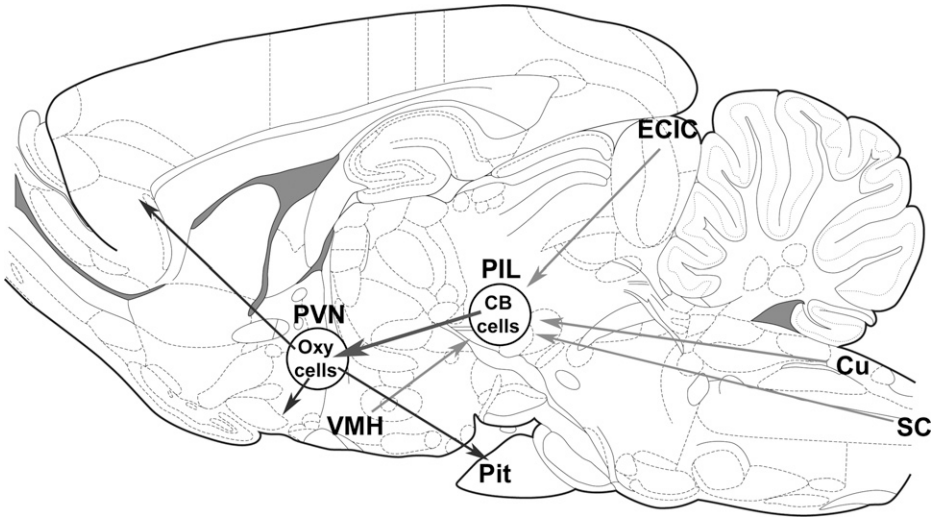

Figure 7. Schematic representation of the neuronal pathway affecting oxytocin neurons (Oxy) in the hypothalamic PVN. Neurons in the spinal cord (SC), the cuneate (and gracile) nucleus (Cu), the external cortex of the inferior colliculus (ECIC), and the ventromedial hypothalamic nucleus (VMH) project to the PIL. CB neurons in the PIL in turn project to the PVN to innervate and excite oxytocin neurons.

Indeed, their extensive social interactions after reunion also argues against anxiety-induced activation of PIL CB neurons. Previous c-Fos studies in social context focused on the social interaction of unfamiliar males in a novel environment as an anxiety test (52, 53). In these circumstances, many brain regions are activated, but an increase in the number of c-Fos–positive cells in the area corresponding to the PIL was not reported. Thus, a role of the PIL-PVN pathway in social interaction–induced oxytocin release (21) is likely, but its involvement in stress-induced oxytocin release (54) cannot be excluded. Nevertheless, our study implicates the PIL in the adult brain social network.

Activation of the PIL has been demonstrated in lactating mothers (22, 23, 55). This study adds that CB neurons of the PIL are activated by pup exposure. The number of c-Fos–containing neurons in the PIL in response to adult social interaction is similar to that seen after suckling in mother rats (23). The neurons activated by suckling may be the relay cells for the milk ejection reflex previously predicted in the ventroposterior thalamic-peripeduncular area (18–20, 56). The similar distribution pattern of c-Fos–positive cells in the PIL after social encounter, as well as the activation of CB neurons following pup exposure in mothers and between familiar adult female conspecifics in a social context, suggests that the same cells may be activated in both conditions. The activation of oxytocin neurons has been described in both situations. In mothers, oxytocin plays a role in milk ejection (57) and in maternal motivation and behavior (3, 4, 58). In adult social contexts, oxytocin release and receptor activation contribute to social recognition and affiliative behavior (6, 9, 59).

Conclusion

In conclusion, oxytocin neurons may be activated by the input from the PIL in different social situations in response to sensory stimuli from other animals. Thus, the PIL-PVN pathway represents a previously missing link in the understanding of how oxytocin neurons can be activated by neuronal inputs. The pathway may contribute to oxytocin release for milk ejection, maternal motivation, social recognition, and affiliation.

Acknowledgments

The authors thank Nikolett Hanák and Szilvia Deák for technical assistance and Karolin M. Suri for technical contribution to the social activation experiment.

Address all correspondence and requests for reprints to: Arpád Dobolyi, PhD, MTA-ELTE NAP B Laboratory of Molecular and Systems Neurobiology, Department of Physiology and Neurobiology, Hungarian Academy of Sciences and Eötvös Loránd University, Budapest 1117, Hungary. E-mail: dobolyia@caesar.elte.hu.

This work was supported by the Postdoctoral Research Fellowship Program of the Hungarian Academy of Sciences (to M.C.), the New National Excellence Program of the Ministry of Human Capacities (to D.K.), OTKA K116538 and KTIA_NAP_B_13-2-2014-0004 research grants (to A.D.), and National Institute of Mental Health Intramural Research Program Grant ZIA-MH002685 (to T.B.U.).

Disclosure Summary: The authors have nothing to disclose.

References

1. Lee HJ, Macbeth AH, Pagani JH, Young WS III. Oxytocin: the great facilitator of life. *Prog Neurobiol*. 2009;**88**(2):127–151.
2. Rich ME, deCárdenas EJ, Lee HJ, Caldwell HK. Impairments in the initiation of maternal behavior in oxytocin receptor knockout mice. *PLoS One*. 2014;**9**(6):e98839.

3. Bosch OJ, Neumann ID. Both oxytocin and vasopressin are mediators of maternal care and aggression in rodents: from central release to sites of action. *Horm Behav*. 2012;**61**(3):293–303.
4. Marlin BJ, Mitre M, D'amour JA, Chao MV, Froemke RC. Oxytocin enables maternal behaviour by balancing cortical inhibition. *Nature*. 2015;**520**(7548):499–504.
5. Strathearn L, Fonagy P, Amico J, Montague PR. Adult attachment predicts maternal brain and oxytocin response to infant cues. *Neuropsychopharmacology*. 2009;**34**(13):2655–2666.
6. Neumann ID. Brain oxytocin: a key regulator of emotional and social behaviours in both females and males. *J Neuroendocrinol*. 2008;**20**(6):858–865.
7. Grinevich V, Knobloch-Bollmann HS, Eliava M, Busnelli M, Chini B. Assembling the puzzle: pathways of oxytocin signaling in the brain. *Biol Psychiatry*. 2016;**79**(3):155–164.
8. Mitre M, Marlin BJ, Schiavo JK, Morina E, Norden SE, Hackett TA, Aoki CJ, Chao MV, Froemke RC. A distributed network for social cognition enriched for oxytocin receptors. *J Neurosci*. 2016; **36**(8):2517–2535.
9. Feldman R, Monakhov M, Pratt M, Ebstein RP. Oxytocin pathway genes: evolutionary ancient system impacting on human affiliation, sociality, and psychopathology. *Biol Psychiatry*. 2016;**79**(3):174–184.
10. Romano A, Tempesta B, Micioni Di Bonaventura MV, Gaetani S. From autism to eating disorders and more: the role of oxytocin in neuropsychiatric disorders. *Front Neurosci*. 2016;**9**:497.
11. Lee MR, Rohn MC, Tanda G, Leggio L. Targeting the oxytocin system to treat addictive disorders: rationale and progress to date. *CNS Drugs*. 2016;**30**(2):109–123.
12. Lefevre A, Sirigu A. The two fold role of oxytocin in social developmental disorders: a cause and a remedy? *Neurosci Biobehav Rev*. 2016;**63**:168–176.
13. Brown CH, Bains JS, Ludwig M, Stern JE. Physiological regulation of magnocellular neurosecretory cell activity: integration of intrinsic, local and afferent mechanisms. *J Neuroendocrinol*. 2013; **25**(8):678–710.
14. Ross HE, Young LJ. Oxytocin and the neural mechanisms regulating social cognition and affiliative behavior. *Front Neuroendocrinol*. 2009;**30**(4):534–547.
15. Pan B, Castro-Lopes JM, Coimbra A. Central afferent pathways conveying nociceptive input to the hypothalamic paraventricular nucleus as revealed by a combination of retrograde labeling and c-fos activation. *J Comp Neurol*. 1999;**413**(1):129–145.
16. Larsen PJ, Mikkelsen JD. Functional identification of central afferent projections conveying information of acute "stress" to the hypothalamic paraventricular nucleus. *J Neurosci*. 1995;**15**(4): 2609–2627.
17. Leng G, Brown CH, Russell JA. Physiological pathways regulating the activity of magnocellular neurosecretory cells. *Prog Neurobiol*. 1999;**57**(6):625–655.
18. Tindal JS. Reflex pathways controlling lactation. *Proc R Soc Med*. 1972;**65**(12):1085–1086.
19. Dubois-Dauphin M, Armstrong WE, Tribollet E, Dreifuss JJ. Somatosensory systems and the milk-ejection reflex in the rat. I. Lesions of the mesencephalic lateral tegmentum disrupt the reflex and damage mesencephalic somatosensory connections. *Neuroscience*. 1985;**15**(4):1111–1129.
20. Hansen S, Köhler C. The importance of the peripeduncular nucleus in the neuroendocrine control of sexual behavior and milk ejection in the rat. *Neuroendocrinology*. 1984;**39**(6):563–572.
21. Uvnäs-Moberg K, Handlin L, Petersson M. Self-soothing behaviors with particular reference to oxytocin release induced by non-noxious sensory stimulation. *Front Psychol*. 2015;**5**:1529.
22. Cservenák M, Bodnár I, Usdin TB, Palkovits M, Nagy GM, Dobolyi A. Tuberoinfundibular peptide of 39 residues is activated during lactation and participates in the suckling-induced prolactin release in rat. *Endocrinology*. 2010;**151**(12):5830–5840.
23. Cservenák M, Szabó ER, Bodnár I, Lékó A, Palkovits M, Nagy GM, Usdin TB, Dobolyi A. Thalamic neuropeptide mediating the effects of nursing on lactation and maternal motivation. *Psychoneuroendocrinology*. 2013;**38**(12):3070–3084.
24. Usdin TB, Hoare SR, Wang T, Mezey E, Kowalak JA. TIP39: a new neuropeptide and PTH2-receptor agonist from hypothalamus. *Nat Neurosci*. 1999;**2**(11):941–943.
25. Dobolyi A, Palkovits M, Usdin TB. The TIP39-PTH2 receptor system: unique peptidergic cell groups in the brainstem and their interactions with central regulatory mechanisms. *Prog Neurobiol*. 2010;**90**(1):29–59.
26. Dobolyi A, Palkovits M, Usdin TB. Expression and distribution of tuberoinfundibular peptide of 39 residues in the rat central nervous system. *J Comp Neurol*. 2003;**455**(4):547–566.
27. Rogers JH, Résibois A. Calretinin and calbindin-D28k in rat brain: patterns of partial co-localization. *Neuroscience*. 1992;**51**(4):843–865.
28. Motomura K, Kosaka T. Medioventral part of the posterior thalamus in the mouse. *J Chem Neuroanat*. 2011;**42**(3):192–209.
29. Coolen LM, Veening JG, Petersen DW, Shipley MT. Parvocellular subparafascicular thalamic nucleus in the rat: anatomical and functional compartmentalization. *J Comp Neurol*. 2003;**463**(2): 117–131.
30. Cruikshank SJ, Killackey HP, Metherate R. Parvalbumin and calbindin are differentially distributed within primary and secondary subregions of the mouse auditory forebrain. *Neuroscience*. 2001;**105**(3):553–569.
31. Dobolyi A, Wang J, Irwin S, Usdin TB. Postnatal development and gender-dependent expression of TIP39 in the rat brain. *J Comp Neurol*. 2006;**498**(3):375–389.
32. Cservenák M, Kis V, Keller D, Dimén D, Menyhárt L, Oláh S, Szabó ER, Barna J, Renner É, Usdin TB, Dobolyi A. Maternally involved galanin neurons in the preoptic area of the rat [published online ahead of print June 14, 2016]. *Brain Struct Funct*.
33. Wang J, Palkovits M, Usdin TB, Dobolyi A. Afferent connections of the subparafascicular area in rat. *Neuroscience*. 2006;**138**(1):197–220.
34. Varga T, Palkovits M, Usdin TB, Dobolyi A. The medial paralemniscal nucleus and its afferent neuronal connections in rat. *J Comp Neurol*. 2008;**511**(2):221–237.
35. Paxinos G, Watson C. *The rat brain in stereotaxic coordinates*. San Diego: Academic Press; 2007.
36. Dobolyi A, Ueda H, Uchida H, Palkovits M, Usdin TB. Anatomical and physiological evidence for involvement of tuberoinfundibular peptide of 39 residues in nociception. *Proc Natl Acad Sci USA*. 2002;**99**(3):1651–1656.
37. Varga T, Mogyoródi B, Bagó AG, Cservenák M, Domokos D, Renner E, Gallatz K, Usdin TB, Palkovits M, Dobolyi A. Paralemniscal TIP39 is induced in rat dams and may participate in maternal functions. *Brain Struct Funct*. 2012;**217**(2):323–335.
38. Szabó ER, Cservenák M, Dobolyi A. Amylin is a novel neuropeptide with potential maternal functions in the rat. *FASEB J*. 2012; **26**(1):272–281.
39. Li C, Chen P, Smith MS. Neural populations in the rat forebrain and brainstem activated by the suckling stimulus as demonstrated by cFos expression. *Neuroscience*. 1999;**94**(1):117–129.
40. Zhou J, Shore S. Convergence of spinal trigeminal and cochlear nucleus projections in the inferior colliculus of the guinea pig. *J Comp Neurol*. 2006;**495**(1):100–112.
41. Coolen LM, Allard J, Truitt WA, McKenna KE. Central regulation of ejaculation. *Physiol Behav*. 2004;**83**(2):203–215.
42. Kiss JZ, Palkovits M, Záborszky L, Tribollet E, Szabó D, Makara GB. Quantitative histological studies on the hypothalamic paraventricular nucleus in rats. II. Number of local and certain afferent nerve terminals. *Brain Res*. 1983;**265**(1):11–20.
43. Qi Y, Namavar MR, Iqbal J, Oldfield BJ, Clarke IJ. Characterization of the projections to the hypothalamic paraventricular and periventricular nuclei in the female sheep brain, using retrograde tracing and immunohistochemistry. *Neuroendocrinology*. 2009; **90**(1):31–53.
44. Larsen PJ, Hay-Schmidt A, Vrang N, Mikkelsen JD. Origin of projections from the midbrain raphe nuclei to the hypothalamic

paraventricular nucleus in the rat: a combined retrograde and anterograde tracing study. *Neuroscience*. 1996;**70**(4):963–988.
45. Williamson M, Viau V. Androgen receptor expressing neurons that project to the paraventricular nucleus of the hypothalamus in the male rat. *J Comp Neurol*. 2007;**503**(6):717–740.
46. Campeau S, Watson SJ, Jr. Connections of some auditory-responsive posterior thalamic nuclei putatively involved in activation of the hypothalamo-pituitary-adrenocortical axis in response to audiogenic stress in rats: an anterograde and retrograde tract tracing study combined with Fos expression. *J Comp Neurol*. 2000;**423**(3):474–491.
47. Dobolyi A, Palkovits M, Bodnár I, Usdin TB. Neurons containing tuberoinfundibular peptide of 39 residues project to limbic, endocrine, auditory and spinal areas in rat. *Neuroscience*. 2003; **122**(4):1093–1105.
48. Faber CA, Dobolyi A, Sleeman M, Usdin TB. Distribution of tuberoinfundibular peptide of 39 residues and its receptor, parathyroid hormone 2 receptor, in the mouse brain. *J Comp Neurol*. 2007;**502**(4):563–583.
49. Dobolyi A, Irwin S, Wang J, Usdin TB. The distribution and neurochemistry of the parathyroid hormone 2 receptor in the rat hypothalamus. *Neurochem Res*. 2006;**31**(2):227–236.
50. Goold CP, Usdin TB, Hoare SR. Regions in rat and human parathyroid hormone (PTH) 2 receptors controlling receptor interaction with PTH and with antagonist ligands. *J Pharmacol Exp Ther*. 2001;**299**(2):678–690.
51. Marina N, Morales T, Díaz N, Mena F. Suckling-induced activation of neural c-fos expression at lower thoracic rat spinal cord segments. *Brain Res*. 2002;**954**(1):100–114.
52. Salchner P, Lubec G, Singewald N. Decreased social interaction in aged rats may not reflect changes in anxiety-related behaviour. *Behav Brain Res*. 2004;**151**(1-2):1–8.
53. Jodo E, Katayama T, Okamoto M, Suzuki Y, Hoshino K, Kayama Y. Differences in responsiveness of mediodorsal thalamic and medial prefrontal cortical neurons to social interaction and systemically administered phencyclidine in rats. *Neuroscience*. 2010; **170**(4):1153–1164.
54. Van de Kar LD, Blair ML. Forebrain pathways mediating stress-induced hormone secretion. *Front Neuroendocrinol*. 1999;**20**(1): 1–48.
55. Lin SH, Miyata S, Matsunaga W, Kawarabayashi T, Nakashima T, Kiyohara T. Metabolic mapping of the brain in pregnant, parturient and lactating rats using fos immunohistochemistry. *Brain Res*. 1998;**787**(2):226–236.
56. Wang YF, Negoro H, Honda K. Effects of hemitransection of the midbrain on milk-ejection burst of oxytocin neurones in lactating rat. *J Endocrinol*. 1995;**144**(3):463–470.
57. Wakerley JB, O'Neill DS, ter Haar MB. Relationship between the suckling-induced release of oxytocin and prolactin in the urethane-anaesthetized lactating rat. *J Endocrinol*. 1978;**76**(3):493–500.
58. Bridges RS. Neuroendocrine regulation of maternal behavior. *Front Neuroendocrinol*. 2015;**36**:178–196.
59. Kent P, Awadia A, Zhao L, Ensan D, Silva D, Cayer C, James JS, Anisman H, Merali Z. Effects of intranasal and peripheral oxytocin or gastrin-releasing peptide administration on social interaction and corticosterone levels in rats. *Psychoneuroendocrinology*. 2016; **64**:123–130.